Polysulfide Anions II: Structure and Vibrational Spectra of the S_4^{2-} and S_5^{2-} Anions. Influence of the Cations on Bond Length, Valence, and Torsion Angle

Omar El Jaroudi,[†] Eric Picquenard,*[,‡] Antoine Demortier,[§] Jean-Pierre Lelieur,[§] and Jacques Corset[‡]

Laboratoire de Dynamique, Interactions et Réactivité, U.M.R. 7075 Université P. & M. Curie, Centre National de la Recherche Scientifique, 2 Rue Henri Dunant 94320 Thiais, France, Université Chouaib Doukkali, Département de Physique, B.P. 20, El Jadida, Maroc, and L.A.S.I.R., Centre National de la Recherche Scientifique-H.E.I., 13 Rue de Toul 59000 Lille, France

Received December 13, 1999

The influence of the cations on bond length, valence, and torsion angle of S_4^{2-} and S_5^{2-} anions was examined in a series of solid alkali tetra- and pentasulfides by relating their Raman spectra to their known X-ray structures through a force-field analysis. The IR and Raman spectra of $BaS_4 \cdot H_2O$ and the Raman spectra of $(NH_4)_2S_4 \cdot nNH_3$, γ-Na_2S_4, and δ-Na_2S_5 are presented. The similarity of spectra of γ-Na_2S_4 with those of $BaS_4 \cdot H_2O$ suggests similar structures of the S_4^{2-} anions in these two compounds with a torsion angle smaller than 90°. The variations of SS bond length, SSS valence angle, and dihedral angle of S_n^{2-} anions are related to the polarization of the lone pair and electronic charge of the anion by the electric field of the cations. A correlation between the torsion angle and the SSS valence angle is shown as that previously reported between the length of the bond around which the torsion takes place and the dihedral angle value. These geometry changes are explained by the hyperconjugation concept and the electron lone-pair repulsion.

Introduction

In a general study of the structure and reactivity of the S_n^{2-} anions in solid metal polysulfides, we examined the influence of the cations on bond length and angle in a series of alkali- and alkaline-earth polysulfides (M_2S_n and $M'S_n$, respectively, with $n = 2$ and 3) by relating their Raman spectra to their known X-ray structures through a force-field analysis.[1] In this article, we extend this analysis to higher polysulfides S_4^{2-} and S_5^{2-} emphasizing on the influence of cations on torsion angle.

It has been shown both experimentally by Hordvik[2] and theoretically by Saethre[3] that the S−S bond length between two divalent sulfur atoms varies with dihedral angle. The curve showing the variation of sulfur(II)−sulfur(II) bond length with dihedral angle displays a minimum around a dihedral angle τ of 90° and a bond length close to 2.03 Å. This variation in bond length with the dihedral angle is assumed to be partly caused by the sulfur atoms lone-pairs repulsion, which is maximum for $\tau = 0°$ and 180° and partly caused by π-bonding arising from the overlap of the pπ electron pair of one divalent sulfur atom with 3d orbitals of a bond partner.[2] Although most of modern quantum chemistry calculations done for sulfur compounds recognize the importance of introducing polarization d orbitals in the basis set,[4−6] their influence is assumed to be small. More recent studies on sulfur−sulfur bonding in sulfanes[7,8] and an older one on cyclic heptasulfur[9] have shown that the concept of hyperconjugation is more relevant than the dπ-pπ one. This hyperconjugation, by which the 3p lone pair of a sulfur atom S(x) is partly delocalized into the empty antibonding σ^* molecular orbital of the adjacent bond S($x + 1$) − S($x + 2$), may influence bond lengths and the torsion angle value close to 90°.

These S(II)−S(II) bond lengths in polysulfide anions range from 2.03 to 2.10 Å. Because such bond lengths are observed in polysulfide anions,[10−18] it is interesting to relate their vibrational spectra to their structure. It is well-known that for a given polysulfide, several crystalline forms may arise according to the preparation method. They can be distinguished by their Raman spectra.

To get a better insight into the relationship between their structure and their spectra, we prepared and recorded spectra of some new compounds. We have obtained new metastable forms of Na_2S_4 and of Na_2S_5. We prepared an ammoniate $(NH_4)_2S_4 \cdot nNH_3$ from liquid ammonia solution. The compound $BaS_4 \cdot H_2O$ was also studied on account of its structure with a dihedral angle of the S_4^{2-} anion much smaller than that in α-Na_2S_4.[10] Our study also is extended to a series of other polysulfides, the structure and spectra of which have been published already: structure: α-Na_2S_4,[10] $BaS_4 \cdot H_2O$,[11,12] and

[†] Université Chouaib Doukkali.
[‡] Centre National de la Recherche Scientifique.
[§] Centre National de la Recherche Scientifique-HEI.

(1) El Jaroudi, O.; Picquenard, E.; Demortier, A.; Lelieur, J.-P.; Corset, J. *Inorg. Chem.* **1999**, *38*, 2394.
(2) Hordvik, A. *Acta Chem. Scand.* **1966**, *20*, 1885.
(3) Saethre, L. J. *Acta Chem. Scand.* **1975**, *A29*, 558.
(4) Quelch, G. E.; Schaefer, H. F.; Marsden, C. J. *J. Am. Chem. Soc.* **1990**, *112*, 8719.
(5) Raghavachari, K.; Rohlfing, C. M.; Binkley, J. S. *J. Chem. Phys.* **1990**, *93*, 5862.
(6) Saethre, L. J.; Gropen, O. *Can. J. Chem.* **1992**, *70*, 348.
(7) Steudel, R.; Drozdova, Y.; Miaskiewicz, K.; Hertwig, R. H.; Koch, W. *J. Am. Chem. Soc.* **1997**, *119*, 1990.
(8) Otto, A. H.; Steudel, R. *Eur. J. Inorg. Chem.* **1999**, 2057.
(9) Steudel, R.; Schuster, F. *J. Mol. Struct.* **1978**, *44*, 143.
(10) Tegman, R. *Acta Crystallogr.* **1973**, *B29*, 1463.
(11) Abrahams, S. C. *Acta Crystallogr.* **1954**, *7*, 423.
(12) Abrahams, S. C.; Bernstein, J. L. *Acta Crystallogr.* **1969**, *B25*, 2365.
(13) Böttcher, P.; Kruse, K. *J. Less-Common Met.* **1982**, *83*, 115.
(14) Böttcher, P. *Z. Kristallografiya* **1979**, *150*, 65.
(15) Kelly, K.; Woodward, P. *J. C. S. Dalton* **1976**, 1314.
(16) Goh, N. K. Dissertation, Münster, 1974.
(17) Böttcher, P.; Keller, R. *Z. Naturforsch.* **1984**, *39B*, 577.
(18) Rosen, E.; Tegman, R. *Acta Chem. Scand.* **1971**, *25*, 3329.

10.1021/ic991419x CCC: $19.00
Published on Web 05/17/2000

Table 1. Wavenumbers (cm^{-1}) of Normal Vibrations of S_4^{2-} Anion for the M_2S_4 and $M'S_4$ Tetrasulfides in Solid State

	Cs_2S_4			K_2S_4		Na_2S_4				$(NH_4)_2S_4 \cdot nNH_3$	$BaS_4 \cdot H_2O$	
	α		γ	γ		α	α		γ			
assignment	R[a,d]	IR[a,d]	IR[a,d]	R[e]	IR[e]	R[f]	R[g]	IR[g]	R[b]	R[b]	R[b]	IR[b]
ν_s	494 ms		483 ms	485 s p	486 sh	482 (4)	483 s	482 m	485 m	487 m	487 m	
ν_a	483 ms	483 sh 473 vs	473 ms	478 sh dp	477	468 (2)	469 ms	469 s	475 m	477 w	470 w	472 m
ν_{cent}	433 s	422 w	422 s	434 s p		445 (10)	445 vs	444 vvw	450 s	449 s	437 s	437 w
δ_a	240 w		250	266 m dp		239 (1)	241 w	242 ms	272 w	245 m	258 m	260 w
δ_s	209 s		195 s	220 m p		206 (3)	212 m	212 m	231 w	200 m	213 w	217 w
τ						83 (1)[c]	98 ms	98 s	88 m	102 w	109 m	

[a] The α-phase is observed at low temperature, and the γ-phase appears after heating at 125 °C. R, Raman scattering; IR, infrared absorption. Intensity: vs, very strong; s, strong; ms, medium strong; m, medium; w, weak; vw, very weak; p, polarized line; dp, depolarized line. [b] This work. [c] Modified assignment. [d] Reference 19. [e] Reference 20. [f] Reference 22. [g] Reference 21.

M_2S_5 (M = Cs,[13] Rb,[14] K,[15] NH_4,[16] Na[17,18]), and spectra: M_2S_4 (M = Cs,[19] K,[20] Na[19,21,22]) and M_2S_5 (M = Cs,[19] Rb,[19] K,[23] NH_4,[16,24] Na[22]).

Experimental Section

The various forms of Na_2S_4 and Na_2S_5 were obtained during an already published study of the reaction between sodium sulfide or disulfide and sulfur.[25] γ-Na_2S_4 was obtained on annealing the glassy form of Na_2S_4 and δ-Na_2S_5 by crystallization of the liquid phase of Na_2S_5. The $BaS_4 \cdot H_2O$ compound was prepared according to the method described by Robinson and Scott.[26] The ammonium tetrasulfide $(NH_4)_2S_4 \cdot nNH_3$ was prepared by reduction of sulfur−ammonia solution by hydrogen sulfide according to the method used by Dubois et al.[27]

The Raman spectra of polysulfide anions at room temperature were recorded with an XY multichannel Dilor instrument equipped with a double monochromator as filter and with a liquid-nitrogen-cooled Wright CCD mosaic detector (1200 × 300). An Olympus microscope was coupled with the XY spectrometer, and a long front objective of magnification (×50) was used to observe the various phases formed in the sealed sample tube. In these conditions, the laser power was kept below 1 mW. The Raman spectra were excited by the 488.0 or 514.5 nm radiations from a Spectra Physics argon ion laser. The infrared spectra were recorded with a Perkin-Elmer 983 spectrometer.

Results

Sodium Polysulfides: Na_2S_4, Na_2S_5. During a Raman study of the reactions of sodium sulfide or disulfide with sulfur, when heated, we have observed that whatever the composition of the mixtures, the solid sodium sulfide or disulfide transforms into the crystalline α-Na_2S_4 in a first step.[25] α-Na_2S_4 is characterized by its Raman spectrum that is very similar to that observed by Janz et al.[22] and Eysel et al.[23] (Table 1). By cooling the mixtures, after heating above 450 °C, a glass is usually obtained characterized by Raman lines with much larger line widths than in a crystalline form (Figure 1b) as already observed by Janz et al.[22] If this glass is annealed further at temperatures between 120 and 200 °C, a new crystalline phase is obtained and is characterized by its Raman spectrum (Figure 1c, Table 1) with line widths similar to those observed for the α-phase. The wavenumbers of its Raman lines are very close to those observed in the glassy state. We have called this new crystalline phase γ-Na_2S_4, by analogy with the γ-phase of Na_2S_5, which is obtained either directly from the melt or by annealing of the Na_2S_5 glass. Further annealing at 200 °C of this metastable phase led to the stable α-Na_2S_4 phase.[25]

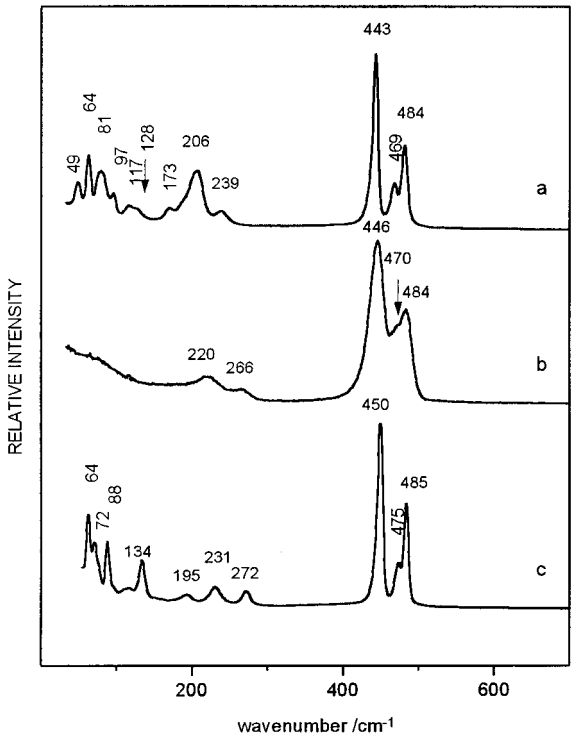

Figure 1. Raman spectra of various forms of Na_2S_4 recorded under the 514.5-nm laser line with a XY DILOR spectrometer. (a) α-Na_2S_4: laser power, 3 mW; slit width, 200 μm (6.23 cm^{-1}); integration time, 30 s. (b) Glassy Na_2S_4: micro sample (×50); laser power, 0.16 mW; slit width, 130 μm (4.05 cm^{-1}); integration time, 600 s. (c) γ-Na_2S_4: laser power, 3 mW; slit width, 210 μm (6.54 cm^{-1}); integration time, 60 s.

Our assignments follow those of Janz et al.[22] for the C_2 site symmetry S_4^{2-} anion in α-Na_2S_4, except for the torsion mode which we assign to the Raman bands at 81 and 88 cm^{-1} for the α- and γ-phase, respectively (Figure 1a and 1c) in better agreement with the results of Eysel et al.[23] for the α-phase. The other bands of smaller intensity at 97, 117, 128, and 173 cm^{-1} for the α-phase and at 134 and 195 cm^{-1} for the γ-phase may in fact be assigned to combination modes or harmonics involving lattice modes.

Similarly, through heating and melting of Na_2S mixtures with sulfur, of overall composition Na_2S_n with $n > 4$, we have observed the α-, β-, glass, and γ-phase of Na_2S_5 already obtained by Janz et al.[22] and a new δ-phase characterized by its Raman

(19) Ziemann, H.; Bues, W. *Z. Anorg. Allg. Chem.* **1979**, *455*, 69.
(20) Janz, G. J.; Coutts, J. W.; Downey, J. R., Jr.; Roduner, E. *Inorg. Chem.* **1976**, *15*, 1755.
(21) Eysel, H. H.; Nöthe, D. *Z. Naturforsch.* **1976**, *31B*, 411.
(22) Janz, G. J.; Downey, J. R.; Roduner, E.; Wasilczyk, G. J.; Coutts, J. W.; Eluard, A. *Inorg. Chem.* **1976**, *15*, 1759.
(23) Eysel, H. H.; Wieghardt, G.; Kleinschmager, H.; Weddigen, G. Z. *Z. Naturforsch.* **1976**, *31B*, 415.
(24) Steudel, R.; Schuster, F. *Z. Naturforsch.* **1977**, *32A*, 1313.
(25) El Jaroudi, O.; Picquenard, E.; Gobeltz, N.; Demortier, A.; Corset, J. *Inorg. Chem.* **1999**, *38*, 2917.
(26) Robinson, P. L.; Scott, W. E. *J. Chem. Soc.* **1931**, 693.
(27) Dubois, P.; Lelieur, J. P.; Lepoutre, G. *Inorg. Chem.* **1988**, *27*, 1883.

Table 2. Wavenumbers (cm^{-1}) of Normal Vibrations of the S_5^{2-} Anions for Alkaline and Ammonium Pentasulfides in Solid State

	Cs_2S_5		Rb_2S_5		K_2S_5		α-Na_2S_5		β-Na_2S_5	γ-Na_2S_5	δ-Na_2S_5	$(NH_4)_2S_5$
	R[c]	IR[c]	R[c]	IR[c]	R[d,e]	IR[e]	R[f]	R[a]	R[f]	R[a]	R[f]	R[b,g]
ν_a	501 m	495 vs br	498 w	495 vs br	496 ms	492 s	488 (3)	486	484 (3.5)	485 (6)	495 m	495 m
ν_s	493 m		489 vw		483 m	477 s				479 (2 sh)	484 m	486 m
ν_s	423 vs	425 sh	427 vs	430 sh	432 vvs		444 (10)	443	444 (10)	451 (10)	433 vs	458 vs
ν_a	415 sh	412 s	417 sh	417 s	421 sh	418 m	391 (0.5)	392	419 (1)	427 (2)	449 w	431 s
δ_a	259 m		262 w		267 m	273 s	266 (2)	265	275 (1)	280 (2)	252 w	272 m 269 sh
δ_s	243 m		246 m		251 m	253 s	214 (2)	214	208 (1)	209(2)	194 m sh	253 m
δ_s	161 m		160		173 m				187 (1)		182 m	169 mw
τ_a	106 m		112		98	97	135 (2)	105	95 (0.5)		104 w	104 s
τ_s			88		77	77	103 (3)	70.5	82 (1)		79 w	68 s

[a] This work. R, Raman scattering; IR, infrared absorption. Intensity: vs, very strong; s, strong; ms, medium strong; m, medium; w, weak; vw, very weak; sh, shoulder; relative intensity in parentheses. [b] Modified assignment. [c] Reference 19. [d] Reference 20. [e] Reference 21. [f] Reference 22. [g] Reference 24.

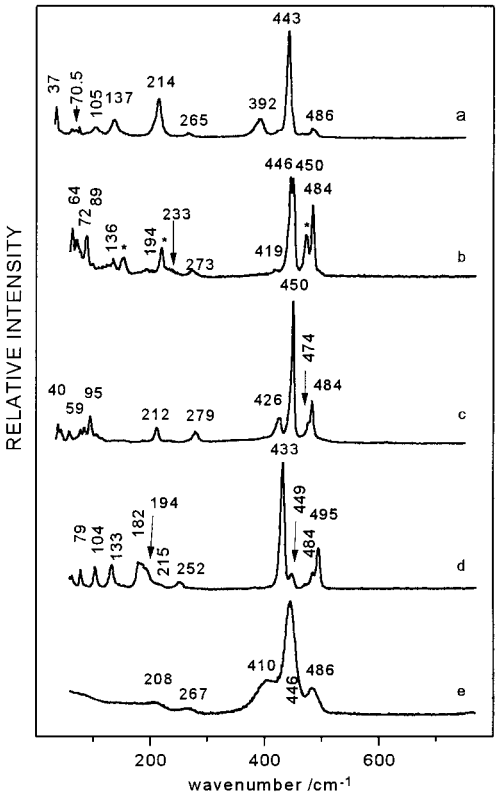

Figure 2. Raman spectra of various forms of Na_2S_5 recorded under the 514.5-nm laser line with a XY DILOR spectrometer. (a) α-Na_2S_5: micro sample (×50); laser power, 0.14 mW; slit width, 120 μm (3.74 cm^{-1}); integration time, 300 s. (b) β-Na_2S_5: micro sample (×50); laser power, 0.075 mW; slit width, 200 μm (6.23 cm^{-1}); integration time, 240 s. * indicates S_8 lines. (c) γ-Na_2S_5: macro sample; laser power, 3 mW; slit width, 100 μm (3.12 cm^{-1}); integration time, 120 s. (d) δ-Na_2S_5: micro sample (×50); laser power, 0.075 mW; slit width, 200 μm (6.23 cm^{-1}); integration time, 600 s. (e) Glassy Na_2S_5: micro sample (×50); laser power, 0.075 mW; slit width, 200 μm (6.23 cm^{-1}); integration time, 600 s.

spectrum (Figure 2a to 2d and Table 2). These compounds where distinguished from their mixtures with Na_2S_4 owing to the use of a Raman microspectrometer. Our assignments, in terms of stretching and bending modes, follow those of Janz et al.[20,22] Our assignment of the torsion mode of α-Na_2S_5 at 105 cm^{-1} is related to the assignment of the band at 137 cm^{-1} to a combination of lattice modes.

Ammonium Tetrasulfide Ammoniate: $(NH_4)_2S_4 \cdot nNH_3$. Through reaction of sulfur with hydrogen disulfide in liquid ammonia, we have obtained the polysulfide $(NH_4)_2S_4 \cdot nNH_3$, after evaporating the ammonia. The Raman spectrum of this compound is shown in Figure 3. Two inserts show the lines

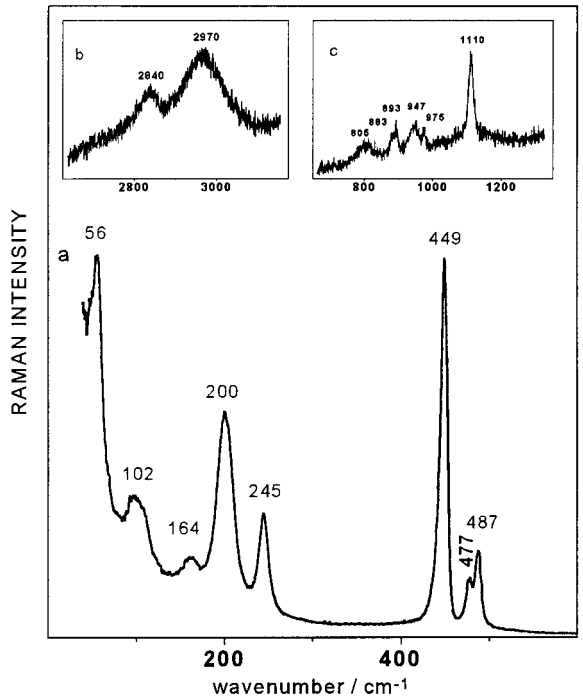

Figure 3. Raman spectra of $(NH_4)_2S_4 \cdot nNH_3$ recorded under the 514.5-nm laser line with a XY DILOR spectrometer. (a) Wavenumber range of S_4^{2-} anion vibration modes: laser power, 1.8 mW; slit width, 200 μm (6.24 cm^{-1}); integration time, 120 s. (b) Wavenumber range of NH_4^+ cation vibration modes: micro sample (×50); laser power, 1.5 mW; slit width, 130 μm (2.95 cm^{-1}); integration time, 600 s. (c) Wavenumber range of NH_3: micro sample (×50); laser power, 1.5 mW; slit width, 130 μm (2.95 cm^{-1}); integration time, 600 s.

belonging to the NH_4^+ cations and to the NH_3-solvating molecules. The left insert shows the stretching vibration region with the $\nu_1(NH_4^+)$ symmetric stretching vibration observed at 2970 cm^{-1} and the $2\nu_4(NH_4^+)$ harmonic of the asymmetric bending vibration at 2840 cm^{-1}. The antisymmetric bending vibration is observed around 1448 cm^{-1} and the $\nu_2(NH_4^+)$ symmetric bending vibration at 1677 cm^{-1}, both not shown. Their wavenumbers are close to those observed for the ammonium chloride ammoniates.[28] The stretching vibration of the solvating ammonia molecules, expected between 3200 and 3400 cm^{-1} as in the $NaBr \cdot 5^1/_7NH_3$ ammoniate,[29] have not be seen. The $\nu_2(NH_3)$ symmetric bending vibration at 1110 cm^{-1} and the $r(NH_3)$ rocking modes between 805 and 975 cm^{-1} (right insert) were also observed, at wavenumbers very close to those

(28) Corset, J.; Huong, P. V.; Lascombe, J. *Spectrochim. Acta* **1968**, *24A*, 2045.
(29) Régis, A.; Limouzi, J.; Corset, J. *J. Chim. Phys.* **1972**, *4*, 699.

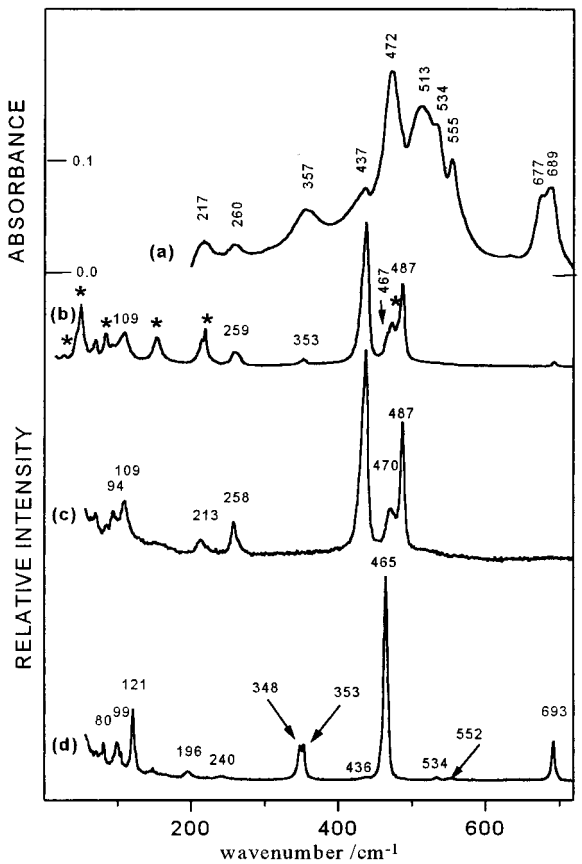

Figure 4. IR and Raman spectra of the mixture of $BaS_4 \cdot H_2O$ with $BaS_2O_3 \cdot H_2O$ and Raman spectra of isolated microcrystals (×50). IR spectra recorded with a Perkin-Elmer 983 spectrometer, Raman spectra with a XY DILOR spectrometer. (a) IR spectrum of Nujol mull of $BaS_4 \cdot H_2O$ and $BaS_2O_3 \cdot H_2O$ mixture. (b) Raman spectrum of $BaS_4 \cdot H_2O$ and $BaS_2O_3 \cdot H_2O$ mixture. Excitation line, 514.5 nm; laser power, 4 mW; slit width, 105 μm (3.23 cm^{-1}); integration time, 20 s. * indicates S_8 lines. (c) Raman spectrum of $BaS_4 \cdot H_2O$. Excitation line, 488 nm; laser power, 0.4 mW; slit width, 70 μm (2.68 cm^{-1}); integration time, 300 s. (d) Raman spectrum of $BaS_2O_3 \cdot H_2O$. Excitation line, 488 nm; laser power, 0.5 mW; slit width, 70 μm (2.68 cm^{-1}); integration time, 600 s.

observed for the $NaBr \cdot 5^1/_7 NH_3$ ammoniate.[29] This confirms the presence of solvating ammonia molecules in this product with *n* probably being small. The strong bands, observed under 500 cm^{-1}, correspond to those of the S_4^{2-} anion in this well-crystallized compound (Figure 1). They are assigned to the central vibration of a C_2 symmetry S_4^{2-} anion as in α-Na_2S_4. Their wavenumbers are in fact very close to somewhat larger intensities for the bending vibrations $\delta_s(S_4^{2-})$ at 200 cm^{-1} and $\delta_a(S_4^{2-})$ at 245 cm^{-1} (Table 1). The bands observed at 56 and 164 cm^{-1} are assigned to lattice modes and harmonic or combination bands.

Barium Tetrasulfide Hydrate: $BaS_4 \cdot H_2O$. The structure of the barium tetrasulfide hydrate, prepared according to the method of Robinson and Scott,[26] was first determined by Abrahams,[11] and later by Abrahams and Bernstein[12] to the precise S−S bond lengths. The orthorhombic crystal of space group $P2_12_12$ contains two S_4^{2-} anions in the unit cell. These two anions, both located on a C_2 axis, are not significantly different, but mainly differ by their surrounding water molecules, one anion (anion 1) having short O..S distances with the terminal sulfur atoms, the other one (anion 2) having short O..S distances with the central sulfur atoms. The IR and Raman spectra of the product we have obtained are shown in Figure 4a and 4b. Figure 4b shows that this product is not pure and contains traces of sulfur in excess characterized by the typical S_8 lines at 50, 84, 154, 219, and 473 cm^{-1}. This Raman spectrum displays also small lines at 353 and 693 cm^{-1} which do not belong to the S_4^{2-} anion. Using a Raman microspectrometer, it is possible to record independently the spectrum of each type of microcrystal forming the powder. Besides traces of sulfur that did not react, a second impurity, probably formed through oxidation of the tetrasulfide anion by air traces, is the barium thiosulfate. Its Raman spectrum, obtained on a microcrystal of this sample, is shown in Figure 4d. The IR spectrum obtained is close to that of $BaS_2O_3 \cdot H_2O$ which has already been published[30] and is reported and compared with our Raman spectrum in Table 3. The Raman spectrum of a microcrystal of $BaS_4 \cdot H_2O$ is shown in Figure 4c. This comparison allows us to show that the strong infrared band observed at 472 cm^{-1} must be assigned to the ν_a(SS) antisymmetric stretching mode of S_4^{2-}, whereas the two symmetric stretching modes of the C_2 symmetry S_4^{2-} anions are observed at 437 (Raman and IR) and 487 cm^{-1} (Raman). The two bending modes of S_4^{2-} are observed at 258 and 213 cm^{-1} in Raman and at 260 and 217 cm^{-1} in IR. Considering the small difference in intensity between these two bands, we assign the Raman band at 258 cm^{-1} to the antisymmetric bending mode and the 213 cm^{-1} band to the symmetric bending mode by analogy with the other tetrasulfides (Table 1). The intense line of low wavenumber at 109 cm^{-1} is assigned to the

Table 3. Comparison of IR and Raman Spectra of $BaS_2O_3 \cdot H_2O$ with Those of the Mixture containing $BaS_4 \cdot H_2O$ as Main Compound (Wavenumbers in cm^{-1})

	$BaS_2O_3 \cdot H_2O$		mixture			
	R[a]	IR[b]	IR[c]	R[d]	R[e]	$BaS_4 \cdot H_2O$
ν_a (SO)	1121 m	1120 1105 1075 } s				
ν_s (SO)	1010 s	1007 988 } s				
δ_s (SO)	693 m	675 s	689 677 } m			
δ_s (SO)	552 w 534 w	556 538 508 } m	555 534 513 } s			
				487 s 473 m	487 s	ν_s (SS) S_4^{2-} ν (SS) S_8
ν (SS)	465 s	468 m 450 w	472 s	467 sh	470 w	ν_a (SS) S_4^{2-}
			437	438 s	437 s	ν_{cent} (SS) S_4^{2-}
		398 sh 366 w				
ν (SSO)	353 348 } m	352 w	357	353 w		
		324 276				
			260	263 m	258 m	δ_a (SSS) S_4^{2-}
	240	250		259		
			217	219		δ (SSS) S_8
					213 w	δ_s (SSS) S_4^{2-}
	196			194		
				154		τ (SSSS) S_8
	121 m					
				109	109 m	τ (SSSS) S_4^{2-}
	99					
					94 w	
	80					

[a] This work, Figure 4d. [b] Reference 30. [c] This work, Figure 4a. [d] This work, Figure 4b. [e] This work, Figure 4c.

(30) Freedman, A. N.; Strauhan, B. P. *Spectrochim. Acta* **1971**, *27A*, 1455.

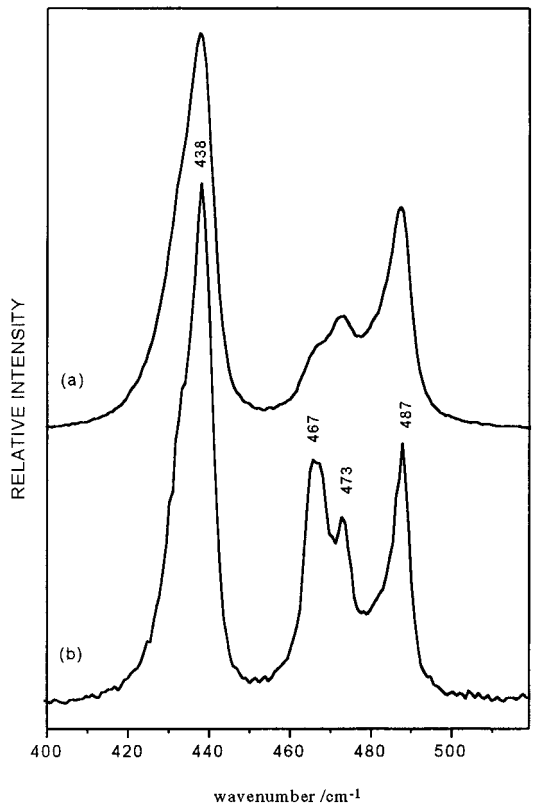

Figure 5. Raman spectra of $BaS_4 \cdot H_2O$ recorded with a XY DILOR spectrometer under the 488-nm laser line (3 mW). (a) Slit width, 100 μm (3.5 cm^{-1}); integration time, 120 s. (b) Slit width, 30 μm (1.05 cm^{-1}); integration time, 300 s.

torsion mode of the S_4^{2-} anion. The small asymmetry on the low wavenumber side of the strong ν_s(SS) Raman line at 437 cm^{-1} could confirm the existence of two anions with a slight difference of geometry in the unit cell. This region of the spectrum has been examined with a better resolution (Figure 5) and a shoulder is clearly seen on the low wavenumber side of the band. The assignment of this shoulder to two types of anion will be discussed later through calculations, because we were unable to obtain a good Raman spectrum at low temperature and high resolution.

Structure and Spectra of the S_4^{2-} Anion. We have summarized in Table 1 the normal mode wavenumbers of the S_4^{2-} anion observed in various alkaline, ammonium, or alkaline-earth salts, indicating their assignment for a S_4^{2-} anion assumed to have C_2 symmetry. It is clear that the three expected stretching vibration modes do not significantly depend on the cation. The lower wavenumber symmetric stretching mode is the most affected one. As already noticed by Ziemann and Bues,[19] the mean stretching wavenumber varies only by 12 cm^{-1} over the range of examined salts. This is in good agreement with the observed bond lengths which are very similar in the two salts of known structure, α-Na_2S_4 and $BaS_4 \cdot H_2O$. If we compare these two salts, the variations of the main band wavenumbers are observed for the bending and torsion vibrations which are appreciably higher in $BaS_4 \cdot H_2O$ than in α-Na_2S_4. Because the S_4^{2-} anion exhibits different SSS angle and dihedral angle in these two compounds, we have calculated the internal valence force field and the normal modes of vibrations for these two types of S_4^{2-} anions of C_2 symmetry. To obtain significant values, we have only refined six force constants to fit the six observed wavenumbers. The stretching force constants f_R (central bond) and f_r (terminal bonds) have been calculated with the Steudel relation[31] from the observed bond length. The stretching−stretching interaction force constant (f_{rr}) referring to bonds with no common atoms and the stretching−torsion interaction force constants ($Rf_{R\tau}$ and $rf_{r\tau}$) have been set arbitrarily at their calculated values in the S_8 force field.[32] The two diagonal force constants, rRf_α for bending and r^2f_τ for torsion, and the four off-diagonal main interaction constants, f_{rR}, $rRf_{\alpha\alpha}$, $Rf_{R\alpha}$, and $rf_{r\alpha}$, have been calculated from the observed geometry and normal vibrations wavenumbers. These results have been summarized in Table 4 and compared with those calculated by Steudel for α-Na_2S_4.[24] The obtained force field is very close to that of Steudel and Schuster[24] except for the two interaction constants, $rf_{r\alpha}$ and $rRf_{\alpha\alpha}$, which are much higher for the first one and have an opposite sign for the second. This fact is evidently related to the use by Steudel and Schuster of two supplementary interaction force constants, rf'_{rr} and $rRf_{\alpha\tau}$. We have calculated, on the same basis, the force field and the wavenumbers of normal modes for the two types of S_4^{2-} anions observed by Abrahams et al.[12] in $BaS_4 \cdot H_2O$. A general increase of the interaction force constant occurs when going from α-Na_2S_4 to $BaS_4 \cdot H_2O$. In addition, it is possible to account for the similarity of observed wavenumbers for the two anions in $BaS_4 \cdot H_2O$ only by decreasing slightly f_{rR} and more significantly $rf_{r\alpha}$, which correspond to the main change in the anion geometry according to the terminal bond r which is lengthened by 0.01 Å. This change in the force field also explains why the lower wavenumber symmetric mode is observed at a slightly lower wavenumber in ion 2 than in ion 1 (Table 4).

The potential energy distribution (PED) obtained with the calculated force field shows that the coupling between the symmetric stretching of the central bond and that of the terminal bonds increases in $BaS_4 \cdot H_2O$ compared with α-Na_2S_4 because of the increase in f_{rR}. The highest wavenumber symmetric stretching vibration is thus essentially related to the central bond in α-Na_2S_4, whereas the symmetric stretching of the terminal bonds predominates in $BaS_4 \cdot H_2O$.

The calculated force field shows an increase of both angle-bending rRf_α and torsion r^2f_τ force constants with the angle closure from 109.76° to 104° for the SSS angle and from 97.81° to 76.5° for the torsion angle, respectively. This is consistent with the observed increase in wavenumbers of both bending and torsion vibrations. It also suggests that the S_4^{2-} anion in γ-Na_2S_4 has a torsion angle smaller than 90° as in $BaS_4 \cdot H_2O$. The sign change of the angle-bending interaction constant is also not unexpected because such changes of sign are usually observed in the force field of *cis*- and *trans*-isomers such as in S_2O_2 [33] or in the tertiobutyl formate where it was assigned to the sign change in the dipole−dipole interaction.[34] Furthermore, the examination of the PED shows that the wavenumber evolution is complicated by the replacement of a slight coupling of the bending motion with the terminal bond stretching motion in α-Na_2S_4 by a coupling with the torsion motion of the bending symmetric motion in $BaS_4 \cdot H_2O$.

Structure and Spectra of the S_5^{2-} Anion. Table 2 summarizes the normal mode wavenumbers known for the various alkaline and ammonium pentasulfides. Their assignments follow that of Steudel and Schuster[24] for a C_2 symmetry anion. Nevertheless the comparison with the other alkaline pentasulfides has led us to assign the antisymmetric torsion motion to the intense band observed for $(NH_4)_2S_5$ at 104 cm^{-1}. The 133

(31) Steudel, R. *Z. Naturforsch.* **1975**, *30B*, 281.
(32) Steudel, R.; Mäusle, H. J. *Z. Naturforch.* **1978**, *33A*, 951.
(33) Marsden, C. J.; Smith, B. J. *Chem. Phys.* **1990**, *141*, 335.
(34) Omura, Y.; Corset, J.; Moravie, R. M. *J. Mol. Struct.* **1979**, *52*, 175.

Table 4. Comparison of Structure, Valence Force Field, and Calculated Normal Mode Wavenumbers (cm^{-1}) of S_4^{2-} Anion of C_2 Symmetry in α-Na_2S_4 and $BaS_4 \cdot H_2O$

	α-Na_2S_4		$BaS_4 \cdot H_2O$	
structure	ref 20		ref 22	
			ion 1	ion 2
central bond				
R, Å	2.061		2.063	2.062
terminal bonds				
r, Å	2.074		2.069	2.079
α(SSS), deg	109.76		104.0	104.3
τ(SSSS), deg	97.81		76.2	76.5
d_m, Å	2.070		2.067	2.073
force field	*a*	ref 9	*a*	*a*
f_R, mdyn Å^{-1}	2.398	2.24	2.380	2.389
f_r, mdyn Å^{-1}	2.290	2.12	2.331	2.251
f_{rR}, mdyn Å^{-1}	0.474	0.48	0.565	0.532
f_{rr}, mdyn Å^{-1}	0.040	0.040	0.040	0.040
$Rf_{r\alpha}$, mdyn	0.276	0.288	0.504	0.504
$rf_{r\alpha}$, mdyn	0.715	0.290	0.517	0.381
rRf_{α}, mdyn Å	1.214	1.239	1.321	1.321
$rRf_{\alpha\alpha}$, mdyn Å	−0.084	0.085	0.057	0.057
r^2f_{τ}, mdyn Å	0.143	0.172	0.282	0.282
rf_{rr}, $rf_{R\tau}$, mdyn	0.124	0.062	0.124	0.124
rf'_{rr}, mdyn		0.040		
$rRf_{\alpha\tau}$, mdyn Å		0.080		

Calculated Normal Mode Wavenumbers (cm^{-1}) PED

	α-Na_2S_4			$BaS_4 \cdot H_2O$	
		PED	ion 1	PED	ion 2
ν_s	484	1.03 f_R, −0.26 f_{rR}, 0.20 ($f_r + f_{rr}$)	487	0.27 f_R, 0.27 f_{rR}, 0.60 ($f_r + f_{rr}$), −0.10 $f_{r\alpha}$	487
ν_a	470	1.03 ($f_r - f_{rr}$)	472	1.08 ($f_r - f_{rr}$), −0.11 $f_{r\alpha}$	471
ν_s	443	0.97 ($f_r + f_{rr}$), 0.13 f_{rR}, −0.20 $f_{r\alpha}$	438	0.96 f_R, −0.49 f_{rR}, 0.55 ($f_r + f_{rr}$), −0.10 $f_{R\alpha}$	432
δ_a	239	1.21 ($f_\alpha - f_{\alpha\alpha}$), 0.17 ($f_r - f_{rr}$), −0.38 $f_{r\alpha}$	258	1.06 ($f_\alpha - f_{\alpha\alpha}$)	260
δ_s	206	1.19 ($f_\alpha + f_{\alpha\alpha}$), 0.18 ($f_r + f_{rr}$), −0.41 $f_{r\alpha}$	216	1.01 ($f_\alpha + f_{\alpha\alpha}$), 0.21$f_\tau$, −0.15 $f_{R\alpha}$, 0.11 $f_{r\alpha}$	217
τ	81	1.06 f_τ	109	0.84 f_τ, 0.14 ($f_\alpha + f_{\alpha\alpha}$)	109

[a] This work.

cm^{-1} band may be assigned to a lattice mode combination (for instance, 81 + 54 = 135 cm^{-1}). In the same way, for α-Na_2S_5 we preferred to relate τ_a to the band observed at 105 cm^{-1} and not to the band at 133 cm^{-1} as Janz et al.[22] reported. For K_2S_5, we followed the assignment by Eysel et al.[23] except for the band at 173 cm^{-1} assigned to a torsion angle by Janz et al.[20] to a torsion. We assign this band to a symmetric bending vibration. The bands observed at 196 and 124 cm^{-1} may be assigned to combination bands. We assign the torsion modes to the bands observed at 98 and 77 cm^{-1}.

The known crystalline structures of alkaline pentasulfides are compared in Table 5. The three Cs, Rb, and K pentasulfides are isotypes with an orthorhombic structure. The S_5^{2-} anion has an helicoidal structure of C_1 symmetry with a motif + + (or − −). This helicoidal structure with a motif + + is kept in the ammonium pentasulfide which crystallizes in the monoclinic system.[16] Although crystallizing in the orthorhombic system, the S_5^{2-} anion in α-Na_2S_5 has a zigzag form with a motif + −.[17] This anion structure also seems present in the β-Na_2S_5 form, which is not so well studied.[17]

As for the S_4^{2-} anion, a great similarity is observed between the spectra of S_5^{2-} anions in alkaline and ammonium pentasulfides. A variation in wavenumber of 14 to 25 cm^{-1} is only observed for each type of stretching vibration mode, if one excepts the lowest antisymmetric stretching mode of the anion S_5^{2-} (+ −) in α-Na_2S_5. Such a similarity is also found for bending vibrations except for the highest wavenumber symmetric bending mode of the anion (+ −), which is observed at a wavenumber approximately 36 cm^{-1} lower than in the other alkaline and ammonium pentasulfides.

Through an a priori change of the G matrix elements without taking into account possible changes of the force constant matrix according to the conformation of the anion, Steudel and Schuster[24] had already shown that the wavenumber variation of the bending modes should reflect these conformation changes. To gain an insight about the relative importance of these two types of parameters, namely geometry and force field, we have calculated the valence force field for the S_5^{2-} anions in alkaline and ammonium pentasulfides. Their structures are known with sufficient accuracy, particularly for the bond length determination, to use the Steudel relation[31] as done for the S_4^{2-} anion. A lengthening of 0.001 Å corresponds to a decrease in the force constant of 0.008 mdyn Å^{-1} according to the Steudel relation. Any inaccuracy in the determination of the bond length may thus make difficult a significant adjustment of the interaction force constants. The adjusted valence force fields to reproduce the observed wavenumbers are shown in Table 5 for the three accurately determined structures, Cs_2S_5, K_2S_5, and α-Na_2S_5. The force field calculated by Steudel for the S_5^{2-} anion with an approximate C_2 symmetry in $(NH_4)_2S_5$ is also given for comparison. These force fields are very close to those obtained for the anion S_5^{2-} (+ +) with the given assumptions. We shall now compare the force field obtained for the anion S_5^{2-} (+ +) in Cs_2S_5 and K_2S_5 with that of the anion (+ −) in α-Na_2S_5. As in S_4^{2-}, for the anion S_5^{2-} (+ +) we have arbitrarily fixed the value of the force constant of the stretching−stretching interaction, between bonds having no common atoms, to the corresponding value found for S_8.[32] For the anion S_5^{2-} (+ −) the value of this constant is increased slightly and an additional small interaction constant between terminal bonds is needed. Apart from the above-mentioned constants, we notice that the stretching−stretching and stretching−bending interaction constants are similar in magnitude. It is not the same for the bending constants and the bending−bending interaction constant. Com-

Table 5. Structure and Valence Force Field of the S_5^{2-} Anion for the M_2S_5 Pentasulfides in Solid State: Calculated Normal Modes Wavenumbers (cm^{-1}) for the Most Accurate Structures

structure[a]	Cs_2S_5	Rb_2S_5	K_2S_5	$(NH_4)_2S_5$		α-Na_2S_5
space group	$P2_12_12_1$	$P2_12_12_1$	$P2_12_12_1$	$P2_1/c$		P_{nma}
type of motif	+ +	+ +	+ +	+ +		+ −
	ref 3	ref 26	ref 12	ref 16		ref 20
r_1, Å	2.032(5)	2.019(7)	2.037(4)	2.058(1)		2.061(2)
R_2, Å	2.077(6)	2.109(7)	2.074(4)	2.073(2)		2.066(2)
R_3, Å	2.070(6)	2.054(8)	2.075(4)	2.054(1)		2.066(2)
r_4, Å	2.022(5)	2.036(8)	2.050(5)	2.059(1)		2.061(2)
α, deg	107.6(2)	109.5(3)	106.4(1)	106.4(1)		108.1(1)
β_2, deg	111.6(2)	107.5(3)	109.7(1)	107.2(1)		107.3(1)
β_4, deg	111.5(2)	111.2(3)	108.7(1)	109.0(1)		107.3(1)
τ_1, deg	75.5	74.5	73.6	67.1		88.6
τ_2, deg	76.9	68.4	68.7	68.0		88.6
d_m, Å	2.050	2.054_5	2.059	2.061		2.063_5
force field					ref 24	
f_{r_1}, mdyn Å^{-1}	2.658[b]		2.611[b]	2.423[b]	2.24	2.398[b]
f_{R_2}, mdyn Å^{-1}	2.267		2.291	2.299		2.359
f_{R_3}, mdyn Å^{-1}	2.323		2.283	2.458		
f_{r_4}, mdyn Å^{-1}	2.754		2.493	2.415		
$f_{R_2r_1}$, mdyn Å^{-1}	0.628		0.600	0.511		0.753
$f_{R_3r_4}$, mdyn Å^{-1}	0.725		0.509	0.785	0.680	
$f_{R_2R_3}$, mdyn Å^{-1}	0.574		0.498	0.520		0.793
f_{Rr_1}, mdyn Å^{-1}	0.040		0.040	0.040	0.030	0.122
$f_{r_1r_4}$, mdyn Å^{-1}						0.093
$Rf_{R\alpha}$, mdyn	0.820		0.640	0.583	0.453	0.651
$Rf_{R\beta}$, mdyn	0.660		0.752	0.480		0.700
$r_1f_{r_1\beta_2}$, mdyn	0.844		0.780	0.755		0.700
$r_4f_{r_4\beta_4}$, mdyn	0.844		0.688	0.605		
$R^2 f_\alpha$, mdyn Å	1.354		1.353	1.307	1.400	1.160
$R^2 f_{\alpha\beta}$, mdyn Å	0.261		0.218	0.200	0.169	0.172
$r_1 R_2 f_{\beta_2}$, mdyn Å	1.060		1.363	1.304		1.088
$r_4R_3f_{\beta4}$, mdyn Å	1.017		1.157	1.222		
r^2f_τ, mdyn Å	0.367		0.279	0.240	0.254	0.313
$rRf_{r\tau}$, mdyn Å	0.117		0.096	0.052		0.010
$Rf_{R\tau}$=$rf_{r\tau}$, mdyn	0.124		0.124	0.124	0.103	0.124
$rRf_{\alpha\tau}$, mdyn Å					0.117	
$rf'_{r\alpha}$, mdyn					0.082	
$rf'_{r\tau}$, mdyn					0.041	
$R^2f_{\beta\beta}$, mdyn Å	0.020					
calcd wavenumber						
ν_a, cm^{-1}	505		496	496		485
ν_s, cm^{-1}	492		483	475		472
ν_s, cm^{-1}	422		432	448		444
ν_a, cm^{-1}	412		418	430		392
δ_a, cm^{-1}	260		270	270		266
δ_s, cm^{-1}	243		252	251		214
δ_s, cm^{-1}	162		173	172		173
τ, cm^{-1}	105		98	105		99
τ, cm^{-1}	86		77	67		82

[a] $r_1 = d_{S(1)S(2)}$; $R_2 = d_{S(2)S(3)}$; $R_3 = d_{S(3)S(4)}$; $r_4 = d_{S(4)S(5)}$; α = S(2)S(3)S(4) angle; β_2 = S(1)S(2)S(3) angle; β_4 = S(3)S(4)S(5) angle. [b] This work.

parison of the anion S_5^{2-} (+ +) in K_2S_5 with the anion S_5^{2-} (+ −) in α-Na_2S_5 shows a large decrease of the bending constant and the bending−bending interaction constant in the anion (+ −). Because the variation of the value of the SSS angle is very small, this decrease in force constant decrease must be related to the increase of the torsion angle from a mean value of 71° for K_2S_5 to a value of 88.6° for α-Na_2S_5. Such a decrease of these force constants was observed for the S_4^{2-} anion, but it was related to the simultaneous increase of both SSS angle and torsion angle. This is also consistent with the small variation of the β-terminal angle bending constant when comparing the anion (+ −) in α-Na_2S_5 with the anion (+ +) in Cs_2S_5, because the β angle increases from 107.3° to 111.5°, whereas the torsion angle decreases from 88.6° to a mean value of 76.2°.

Structure and Force-Field Dependence of the S_4^{2-} and S_5^{2-} Anions on the Cation Electric Field. It is first important to notice that the relation found by Hordvik[2] for disulfides and extended by Steudel[35] to homocyclic sulfur molecules is approximately valid for charged SS bonds in S_4^{2-} and S_5^{2-} as shown in Figure 6. The data points for α-Na_2S_4 and $BaS_4{\cdot}H_2O$, corresponding to a same value of central bond length, are thus located on each side of the minimum. Furthermore, this central bond is always shorter than the terminal ones. Two different concepts may explain this phenomenon: on one hand, the hyperconjugation concept[8] which involves the delocalization of the 3p lone pair of one S atom into the antibonding σ^* molecular orbital of the neighboring bond; on the other hand, the partial localization of the electronic charge into the highest occupied molecular orbital, that is antibonding, for the S_4^{2-} anion.[4,36]

In the hyperconjugation concept, the interactions of both the lone-pair orbitals of terminal atoms with the antibonding σ^* molecular orbital of the central bond and the lone-pair orbitals of central atoms with the antibonding σ^* molecular orbitals of terminal bonds must be considered. For α-Na_2S_4, the large value

(35) Steudel, R. *Z. Naturforsch.* **1983**, *38B*, 543.
(36) Foti, A. E.; Smith, V. H., Jr.; Salahub, D. R. *Chem. Phys. Lett.* **1978**, *57*, 33.

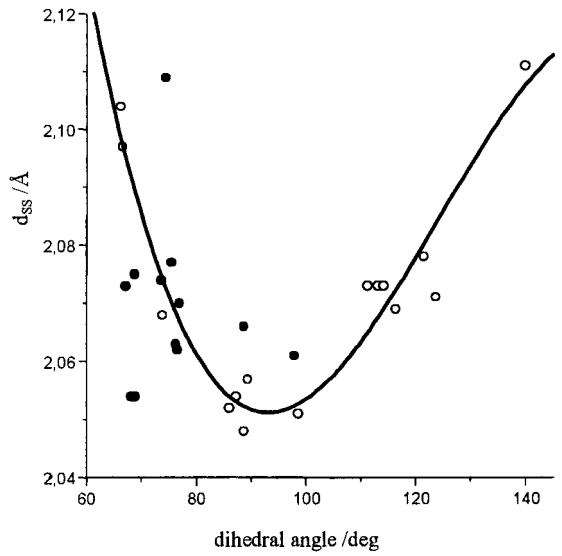

Figure 6. The variation of sulfur−sulfur bond length (d_{SS}) with dihedral angle. ●, polysulfide anions; ○, homocyclic sulfur molecules from ref 35.

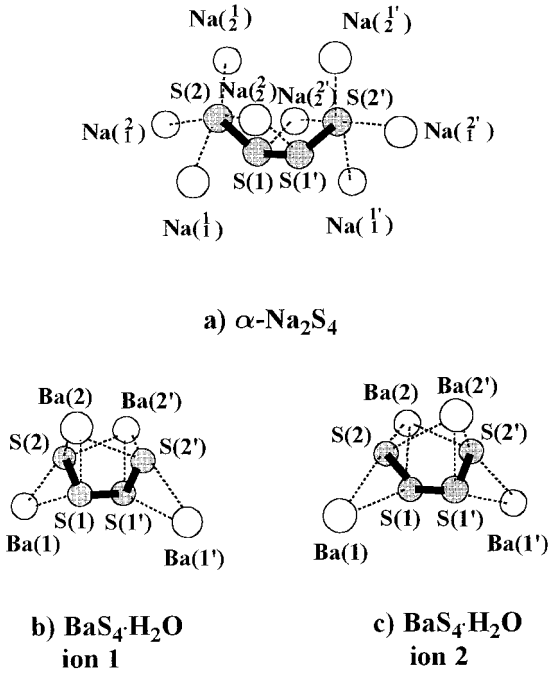

Figure 7. Neighboring cations at a short distance from the S_4^{2-} anion in the unit cell of the tetrasulfides α-Na_2S_4 and $BaS_4 \cdot H_2O$. For the MS distances see Table 6.

of the torsion angle $\tau = 97.9°$ may explain the small central bond length owing to a weak repulsion of lone pairs of S(1) and S(1′) atoms but is also due to the hyperconjugation between the 3p lone pair of these atoms and the antibonding σ^* molecular orbitals of the terminal bonds, which is in line with the bond length difference observed between the central and terminal bonds. The spatial distribution of Na cations at short distances from the sulfur atoms of S_4^{2-} is shown in Figure 7a and Table 6. The polarization of the 3p lone pairs of terminal atoms S(2) and S(2′) by the Na cations at short distances should, in these conditions, disadvantage their hyperconjugation with the S(1)−S(1′) σ^* orbital. The $Na\binom{2}{2}$ and $Na\binom{2'}{2}$ cations, responsible for the closure of the S(2)S(1)S(1′) and S(2′)S(1′)S(1) angle, are at a greater distance (0.17 Å) from sulfur atoms than similar cations [Na(7) and Na(8)] in $Na_2S_3 \cdot NH_3$.[1] This greater distance

Table 6. Short MS Distances (Å) in the Cationic Environment of the S_4^{2-} Anion in the α-Na_2S_4 and $BaS_4 \cdot H_2O$ Crystal Unit Cells and Sum of Crystal Ionic Radii (Å)

α-Na_2S_4		$BaS_4 \cdot H_2O$		
			ion 1	ion 2
$Na\binom{1}{1}$ S(2), $Na\binom{1'}{1}$ S(2′)	2.842	Ba(1)S(1), Ba(1′)S(1′)	3.616	3.317
$Na\binom{2}{1}$ S(2), $Na\binom{2'}{1}$ S(2′)	2.887	Ba(1)S(2), Ba(1′)S(2′)	3.356	3.276
$Na\binom{1}{2}$ S(2), $Na\binom{1'}{2}$ S(2′)	2.826	Ba(2)S(1), Ba(2′)S(1′)	3.491	3.551
$Na\binom{2}{2}$ S(2), $Na\binom{2'}{2}$ S(2′)	3.084	Ba(2)S(2), Ba(2′)S(2′)	3.250	3.313
$Na\binom{2}{2}$ S(1′), $Na\binom{2'}{2}$ S(1)	3.043	Ba(2)S(2′), Ba(2′)S(2)	3.464	3.472
$r_{Na^+} = r_{S^{2-}}$ [a] = 2.82		$r_{Ba^{2+}} = r_{S^{2-}}$ [a] = 2.82		

[a] Crystal ionic radii from ref 38.

is in line with the opening of the angle from 106.5° in $Na_2S_3 \cdot NH_3$ [1] to 109.7° in α-Na_2S_4. A similar explanation holds for the S_4^{2-} anion in $BaS_4 \cdot H_2O$ (Figure 7b and c) for which a closure of both torsion angle and SSS angle is observed owing to the interaction of cations Ba(2) and Ba(2′), both with the two terminal sulfur atoms S(2) and S(2′), which are a relatively short distance from these cations. The large polarization of the 3p lone pairs of S(2) and S(2′) atoms by the Ba cations may balance the increase of repulsion of the lone pairs of central sulfur atoms induced by the closure of torsion angle. Comparison of anions 1 and 2 in $BaS_4 \cdot H_2O$ must take into account the localization of the electronic charge in the antibonding orbitals of terminal bonds (Figure 7b and 7c and Table 6). Indeed, the Ba(1) or Ba(1′) cations are closer to S(1) or S(1′) by 0.3 Å and to S(2) or S(2′) by 0.08 Å, respectively, in ion 2 than in ion 1. This favors the electronic charge localization on the S(1)−S(2) or S(1′)-S(2′) bonds which are 0.01 Å shorter in ion 2 than in ion 1. Molecular orbital calculations for S_4[4,36] and S_2O_2[33] showed that the lowest unoccupied molecular orbital (LUMO) is π^* antibonding on all atoms in the plane C_{2v} conformation, but almost only antibonding on the terminal bonds in a C_2 conformation.[33,36] Thus the localization of the electronic charge in this orbital in S_4^{2-} explains the lengthening of terminal bonds compared with the central bond. The distinction between hyperconjugation and electronic charge localization could then be based only on the more or less pronounced σ^* or π^* character of the S_4^{2-} highest occupied molecular orbital (HOMO). As pointed out by Foti et al.,[36] the $\sigma-\pi$ distinction of the character of this orbital no longer exists on going from the C_{2v} to C_2 conformation.

The helicoidal anion S_5^{2-} in Cs_2S_5 (− −) and K_2S_5 (+ +), shown as an example in Figure 8b and 8c and Table 7, has no cation at a short distance from its central sulfur atom S(3). The 3p lone pair of this atom may contribute to the hyperconjugation with the antibonding σ^* molecular orbital of both terminal bonds. On the opposite, unless the polarization of the lone pairs of terminal atoms S(1) and S(5), as well as S(2) and S(4) atoms by the cations at short distance, the lone pairs of these atoms may contribute to the hyperconjugation with the σ^* molecular orbitals of central bonds. This last hyperconjugation, taking into account the number of lone pairs, becomes predominant over the previous one contrary to what is encountered in S_4^{2-}. This explains that the central bonds are longer than the terminal ones.

The S_5^{2-} anion in α-Na_2S_5 has C_s symmetry with a motif + − (Figure 8a). We noticed that each sulfur atom is interacting with at least one Na cation at short distances (Table 7). The lone pairs of all sulfur atoms are thus polarized by these Na cations decreasing the hyperconjugation. Only a small difference of length between central and terminal bonds is observed (Table

Table 7. Short MS Distances (Å) and SSM Angle (deg) in the Cationic Environment of the S_5^{2-} Anion in the α-Na_2S_5, K_2S_5, and Cs_2S_5 Crystal Unit Cells and Sum of Crystal Ionic Radii (Å)

α-Na_2S_5		K_2S_5		Cs_2S_5	
$Na(^1_1)$ S(1), $Na(^{1'}_1)$) S(5)	2.883	K(1)S(1)	3.322	$Cs(^1_1)$ S(1)	3.592
$Na(^3_1)$ S(1), $Na(^{3'}_1)$S(5)	2.913	K(2)S(1)	3.365	$Cs(^2_1)$ S(1)	3.575
$Na(^1_2)$ S(1), $Na(^1_2)$ S(5)	2.856	K(2)S(2)	3.358	$Cs(^2_1)$ S(4)	3.526
$Na(^2_2)$ S(2), $Na(^2_2)$ S(5)	3.015	K(3)S(1)	3.317	$Cs(^3_1)$ S(1)	3.507
$Na(^2_2)$ S(2), $Na(^2_2)$ S(4)	3.022	K(4)S(1)	3.284	$Cs(^3_1)$ S(2)	3.605
$Na(^2_1)$ S(2), $Na(^{2'}_1)$ S(4)	3.024	K(4)S(2)	3.422	$Cs(^3_1)$ S(5)	3.507
$Na(^3_2)$ S(3)	2.953	K(4)S(4)	3.376	$Cs(^1_2)$ S(1)	3.633
		K(4)S(5)	3.328	$Cs(^1_2)$ S(2)	3.618
		K(1′)S(5)	3.293	$Cs(^2_2)$ S(5)	3.435
		K(2′)S(5)	3.216	$Cs(^3_2)$ S(5)	3.550
		K(3′)S(5)	3.326	$Cs(^3_2)$ S(2)	3.618
		K(4′)S(5)	3.470	$Cs(^4_2)$ S(5)	3.631
S(2)S(1) $Na(^1_1)$	109.2	S(2)S(1)K(1)	104.7	S(2)S(1) $Cs(^1_1)$	84.1
S(2)S(1) $Na(^3_1)$	108.8	S(2)S(1)K(2)	72.2	S(2)S(1) $Cs(^2_1)$	104.8
S(2)S(1) $Na(^1_2)$	105.9	S(2)S(1)K(3)	87.7	S(2)S(1) $Cs(^1_2)$	73.3
S(2)S(1) $Na(^2_2)$	70.2	S(2)S(1)K(4)	76.1	S(4)S(5) $Cs(^2_2)$	80.7
		S(4)S(5)K(1′)	110.7	S(4)S(5) $Cs(^3_2)$	109.8
		S(4)S(5)K(2′)	117.5	S(4)S(5) $Cs(^4_2)$	79.8
		S(4)S(5)K(3′)	81.3		
		S(4)S(5)K(4′)	78.9		
$r_{Na^+} + r_{S^{2-}}$ [a] = 2.82		$r_{K^+} + r_{S^{2-}}$ [a] = 3.18		$r_{Cs^+} + r_{S^{2-}}$ [a] = 3.52	

[a] Crystal ionic radii from ref 38.

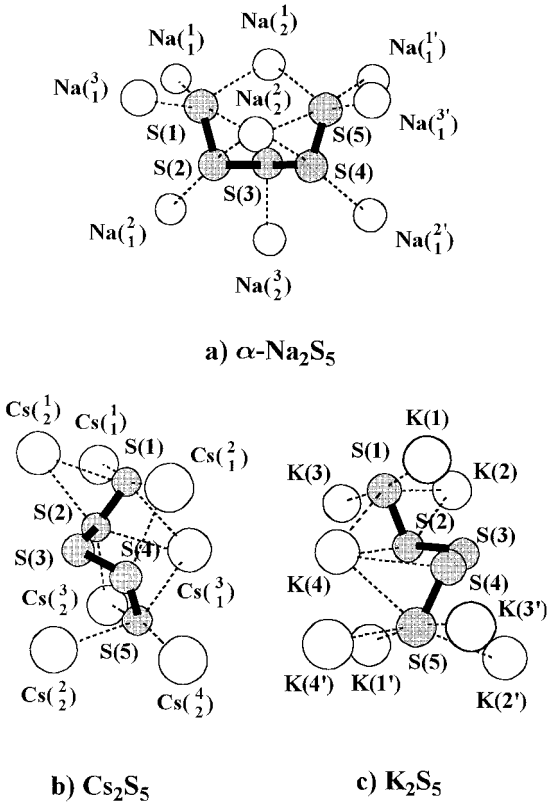

Figure 8. Neighboring cations at short distance of the S_5^{2-} anion in the unit cell of the alkaline pentasulfides α-Na_2S_5, Cs_2S_5, and K_2S_4. For the MS distances see Table 7.

5). Although stability of S_n^{2-} anions has been studied by ab initio methods[37] no detailed molecular orbital calculations are known for S_5^{2-}. The difference of length of central bonds in S_5^{2-} anions of C_{2v} symmetry and helicoidal may also be explained by a localization of the electronic charge in the antibonding orbitals of these bonds. Thus, in α-Na_2S_5, the electronic charge will be delocalized in the overall anion. According to the above-mentioned hypothesis, the bond length d_{SS} that decreases with the cation polarizing power for S_3^{2-} from 2.12 to 2.05 Å,[1] also decreases with the number of bonds in the S_n^{2-} anions, if we consider the mean bond length. This mean bond length varies between 2.073 and 2.067 Å for S_4^{2-} and between 2.063 and 2.050 Å for S_5^{2-}. This seems to indicate that the longer the sulfur chain, the smaller the localization of electronic charge in antibonding orbitals influences the mean bond length, thus stabilizing the anion,[37] or that in the hyperconjugation concept the π-type bonding predominates in the lone-pair delocalization mechanism.

These results are also confirmed by our force-field calculation results. In Figure 9, we have plotted the SSS α-angle for S_4^{2-} and central α-angle and β-terminal angle for S_5^{2-}, their corresponding bending force constants, R^2f_α and rRf_β, and the torsion force constant, r^2f_τ, versus the value of the dihedral angle τ. Figure 9a shows all α-angles decrease as τ decreases for the most symmetrical structures α-Na_2S_4, $BaS_4{\cdot}H_2O$, and α-Na_2S_5. A steeper decrease is observed for most β-angles as τ decreases. The α-angles for the S_5^{2-} helicoidal anions lie between the two limit lines. The variation of the torsion force constant shows a maximum (Figure 9c) for a value of τ close to the value found for the minimum of d_{SS} bond length in agreement with a certain π character of this bond close to the minimum (Figure 6). Conversely, the variation of the bending force constant shows

(37) Berghof, V.; Sommerfeld, T.; Cederbaum, L. S. *J. Phys. Chem. A* **1998**, *102*, 5100.
(38) *Handbook of Chemistry and Physics*, 46th ed.; Weast, R. C., Selby, S. M., Hodgman, C. D., Eds.; The Chemical Rubber Co.: Cleveland, OH, 1965−1966; p F 117.

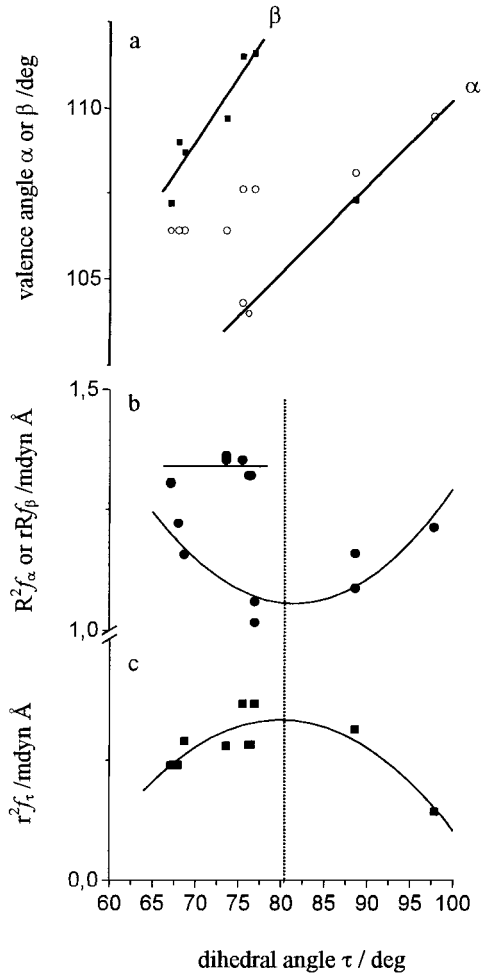

Figure 9. Variations with the dihedral angle for S_4^{2-} and S_5^{2-} anions in the M_2S_n and $M'S_n$ polysulfides of: (a) valence angles α (○) and β (□); (b) bending force constants R^2f_α or rRf_β (◆); (c) torsion force constant r^2f_τ (■).

a minimum (Figure 9b). On the high-τ-value side of the minimum, there is no difference between the central α-angle and external β-angles in the anion S_5^{2-} (+ −) in α-Na_2S_5. The bending force constant decreases with τ decrease as expected with the increase of the hyperconjugation when τ approaches the minimum value. On the low-τ-value side of the minimum, the two angles on each side of the bond, around which the torsion takes place, behave differently. The force constant rRf_β for β-angles in S_5^{2-} anions mostly increases as τ decreases because of the decrease of hyperconjugation and the closure of α-angle. Surprisingly, the force constant r^2f_α of the central α-angle in S_5^{2-} has a high value close to 1.35 mdyn Å, as in $BaS_4{\cdot}H_2O$, and does not seem to be altered by τ variation. This constant value seems to indicate that the decrease of the hyperconjugation is compensated by the lone-pair repulsion which increases as τ decreases.

We have plotted in Figure 10 the stretching−stretching interaction constant between two neighboring bonds versus their corresponding mean bond length value d_m. Figure 10 demonstrates that this interaction force constant increases linearly as the d_m value decreases, as already noticed for the S_3^{2-} anion.[1] This is ascribed to a more pronounced interaction of the 3p lone-pair orbitals of an S atom with the antibonding σ^* orbital of the neighboring SS bond.

It seems that we can draw a curve (Figure 11) similar to that found for the S_3^{2-} anions, plotting the volume left free for the S_5^{2-} anion by the cations in the unit cell $V_{S_5^{2-}}$ versus the

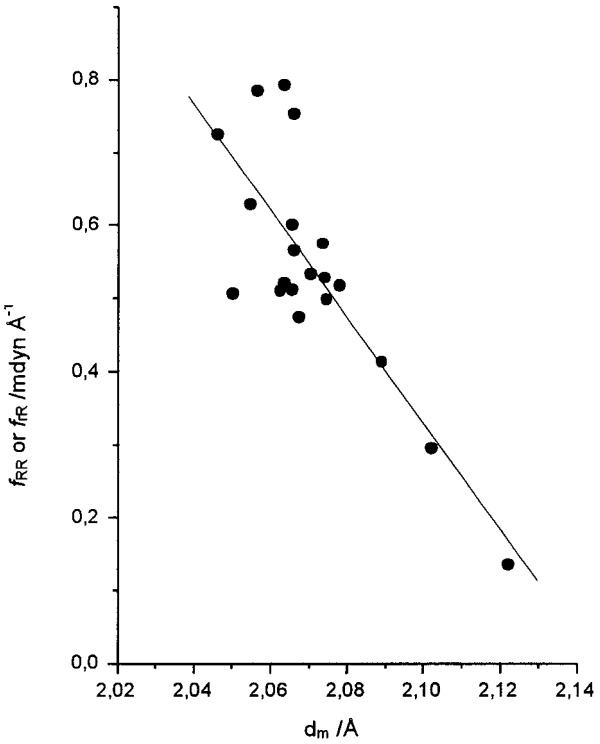

Figure 10. Variations of the stretching−stretching interaction force constants with the mean bond length d_m for S_3^{2-}, S_4^{2-}, and S_5^{2-} anions in the M_2S_n and $M'S_n$ polysulfides.

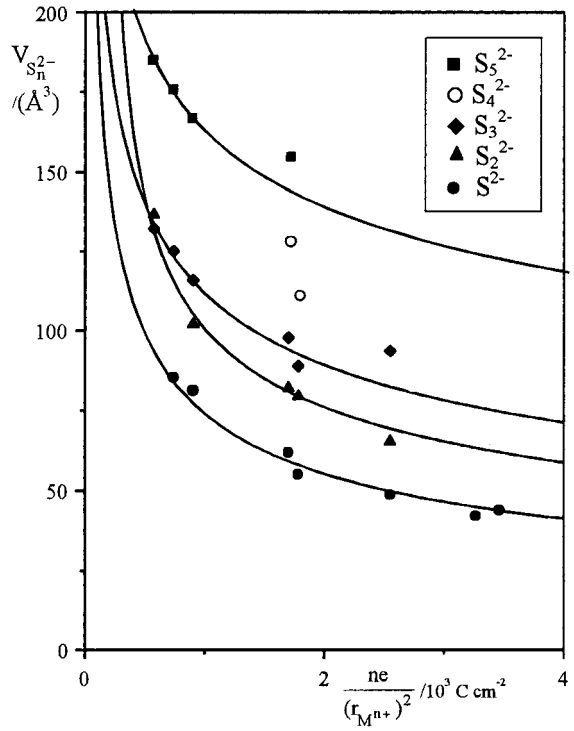

Figure 11. Volume left free for the S^{2-}, S_2^{2-}, S_3^{2-}, S_4^{2-}, and S_5^{2-} anions in the unit cell versus the polarizing power of the cation.

electric field of the cations $ne/(r_{M^{n+}})^2$. In the S_4^{2-} anion, where we have only two points, a volume difference of about 16 Å^3 is observed. The S_4^{2-} anion in $BaS_4{\cdot}H_2O$, which has a small torsion angle, has the smaller expected volume. The high value found for $V_{S_5^{2-}}$ in α-Na_2S_5 compared with the line drawn parallel to that found for S_3^{2-} shows that the lone-pair electron in the motif + − with a large torsion angle as in α-Na_2S_4 is much more bulky.

Conclusion

Through comparison of the vibrational spectra and the X-ray structures of prepared compounds and reported data, it is shown that the geometry changes of the S_n^{2-} anions may be related to the cation electric field of alkaline, ammonium, and alkaline-earth cations. This polarizing effect, which is very large for the volume of the S^{2-} anion, decreases with n for the S_n^{2-} anions. The position of cations at short distances is responsible for the variation of the bond length, valence angle, and torsion angle in relation to the hyperconjugation of the 3p lone-pair orbital of a S(x) atom with the antibonding σ^* molecular orbital of the S($x + 1$) − S($x + 2$) bond, or to the lone pairs repulsion and the electronic charge delocalization. These explanations are in good agreement with the force constant variations with the geometry of S_n^{2-} anions.

The S_4^{2-} anion structure change observed when heating the melt with the overall Na_2S_4 composition probably corresponds to the dissociation of ionic aggregates where the cation repulsion prevents the torsion angle closure as in α-Na_2S_4 and yields a more stable ion pair S_4Na^- with a Na^+ ion bridging the terminal S(2) atoms. This S_4^{2-} anion has in S_4Na^- a torsion angle smaller than 90° as in γ-Na_2S_4 and $BaS_4 \cdot H_2O$.

Acknowledgment. The authors thanks one of the referees for pointing out the importance of the hyperconjugation model in the explanation of the geometry variations of S_n^{2-} anions.

IC991419X